CHAPTER 4

AN IMPROVISED OPTICAL REFRACTOMETER

4.1 INTRODUCTION

The determination of the refractive index (RI) is very important in industries, particularly in chemical and pharmaceutical industries. The measure of refractive index would provide information about the turbidity of a liquid [46]. The measurement of Refractive indices in liquids is challenging using optical fibre. Research has been progressing in this field and many optical methods has been proposed and developed for the measurement of refractive index of liquids. The details of some work on RI have already been discussed in Chapter 1 [7-23] and, so those works are not discussed again in this chapter.

The measurement of Refractive Index (RI) is commonly carried out using a Refractometer [8-20, 22]. Apart from the work given in literatures cited in chapter 1, other types of refractometers have also been reported. Kumar, A., *et al.* [27] fabricated a refractometer using a bare and tapered multimode fibre that can be used to find out the refractive index of different liquids. Villatoro, J., *et al.* [47] proposed an optical refractive sensor based on the radiation losses introduced by the sample medium in an uncladded multimode tapered fibre to measure the refractive index of different liquids. Takeo and Hattori, J., [48] reported an optical fibre based refractometer based on the measurement of input and output optical power. Banerjee, A., *et al.* [49] showed that an optical fibre, partially stripped of its cladding can sense refractive index of a liquid in which the uncladded sensing region is immersed, to a high degree of precision and over a wide range of refractive index. Cusano, A. *et al.* [50] proposed an optical fibre refractometer using a single mode fibre, source, detector and Y coupler to find the refractive index of liquid.

Wu, P., *et al.* [51] modelled a Single mode nanowire sensor employing a wire-assembled Mach-Zehnder structure. In the sensor the phase change originates from the change of refractive index of the medium surrounding the nanowire.

Viegas, J., *et al.* [52] demonstrated an integrated optical refractometer based on multimode interference, with sensitivity enhancement due to sub-micrometer axial features. St-Gelais, R., *et al.* [53] proposed a high resolution, robust and low cost integrated refractometer for microfluidic systems. The device is made of two Bragg reflectors vertically etched in silicon to form an in-plane Fabry-Perot filter. Liquids are injected in the cavity through a microfluidic channel and the variation of the refractive index induces a shift of the resonance wavelength.

Turin, J., *et al.* [54] demonstrated a flexible fibre optic refractometer and its experimental evaluation. Two types of fibre optic refractometers are considered: a basic fibre optic refractometer (based on the use of one fibre optic transducer) and a most sophisticated differential fibre optic refractometer. Lu, Y-C., *et al.* [55] constructed a refractometer based on the polarization effects in tilted fibre Bragg grating (TFBG).

Zhu, T., *et al.* [56] made simultaneous measurement of RI and temperature using a single ultra-LPFG with period up to several millimeters. Lu, P., *et al.* [57] proposed an approach to achieve simultaneous measurement of refractive index and temperature using a Mach–Zehnder interferometer realized on tapered single-mode optical fibre.

Sun, J., *et al.* [58] used Photonic crystal has also been used for the measurement of refractive index. Veldhuis, G.J., *et al.* [59] reported a refractometer, based on measuring the throughput of a bent channel waveguide. This waveguide, designed in SiON technology makes the throughput strongly dependent on the refractive index of a measurand fluid. This new waveguide can be designed for any measurand refractive index ranges from 1.00 - 2.00. Govndan, G., *et al.* [60] presented a refractometer to determine the refractive index of liquids using reflective type fibre optic displacement sensor consisting of two multimode step index fibres and a mirror. Sun, H., *et al.* [61] proposed an optical fibre sensor with simple multimode fibre (MMF)–dispersion compensation fibre (DCF)–multimode fibre structure based on Mach–Zehnder Interferometer (MZI) and studied its

temperature and refractive index (RI) sensing characteristics. The sensing principle is based on the interference between core and cladding modes of DCF due to the large core diameter mismatch. Chiu, M-H., *et al.* [62] proposed a new type of fibre optic sensor (FOS) based on total-internal reflection heterodyne interferometry (TIRHI) which can be used as a liquid refractometer.

Liang, W., *et al.* [63] used fibre Bragg grating technology with a wet chemical etch-erosion procedure to demonstrate two types of refractive index sensors using single-mode optical fibres. The first index sensor device is an etch-eroded single FBG with a radius of 3mm, which is used to measure the indices of four different liquids. The second index sensor device is an etch-eroded fibre Fabry-Pérot interferometer with a radius of, 1.5mm and is used to measure the refractive indices of isopropyl alcohol solutions of different concentrations.

Chen, J., *et al*. [64] proposed an optical fibre refractometer sensor based on the evanescent higher order modes and this sensor is composed of two segments of optical fibres that are spliced together. The attenuation peak wavelength of the interference with specific order in the transmission spectrum shifts with changes in the environmental refractive index and temperature.

The refractometers developed by researchers have been utilized for the measurement of other parameters. Lam, C.C.C., *et al.* [65] showed the application of refractometer for measurement of chloride ions in solutions. A reflective, gold-coated long period grating-based sensor has been developed for the purpose and the sensor was calibrated and evaluated in the laboratory using sodium chloride solutions, over a wide range of concentrations, from 0.01 to 4.00. M. Patil and Shaligram, A. D., [66] proposed a refractometer using parallel two fibre sensor probe consisting transmitting fibre and receiving fibre with a reflector is used as a sensor to test the adultration in diesel. In yet another application, a refractometer based on the intensity-modulated intrinsic fibre optic sugar sensor has been presented. Kumar, A.J, *et al.* [67] used a refractometer in which a portion of an optical fibre is removed and the uncladded portion is immersed in different concentration of sugar solution to determine the refractive index of the solution.

Based on the design of the uncladded and tapered multimode fibre as shown by Kumar, A., *et al.*[27] and Villatoro, J., *et al.* [47] and using the theoretical background of Kumar, A., *et al.*[27], an improved optical fibre refractometer along with its instrumentation system has been proposed in this chapter.

This chapter presents an improved optical fibre refractometer to measure the RI of an unknown liquid. A bare, tapered and bent multi-mode optical fibre (BTBMOF) is used as refractometer to construct an optical fibre sensor probe (OFSP). The modified refractometer would enhance the sensitivity of the proposed micro-controller based instrumentation system used for the measurement of RI of an unknown liquid. The BTBMOF is used to fabricate an OFSP, using a Diode laser source (with a pigtail) and a LDR as a detector. Laser beam from the Diode laser Source is launched at one end of the BTBMOF. The power transmitted through the bare, tapered and bent portion of the multi-mode optical fibre depends on the RI of the liquid applied around it. The laser beam propagating through the BTBMOF is applied on the surface of the LDR. The resistance value of the LDR changes according to the change in RI value of the liquid surrounding the BTBMOF. The LDR is connected across a 5V supply with a series resistance to form a potential divider circuit. The output from the potential divider circuit is interfaced to the ADC0 (analog input pin 0) of an ATmega 32 microcontroller via a passive low-pass filter for reading and displaying the RI value of the liquid.

4.2 FUNDAMENTAL OPERATING PRINCIPLE OF THE IMPROVED REFRACTOMETER

4.2.1 Principle of Bare, Tapered and Bent Multimode Refractometer:

The design of bare, bent and tapered multimode optical fibre (BTBMOF) is derived from the bare and tapered multimode fibre as discussed in Chapter 2 Section 2.4. The bare and tapered portion of the optical fibre sensor is given a shape of a semicircular arc of fixed radius of curvature to construct the BTBMOF portion of the optical fibre sensor probe (OFSP). The geometry of the proposed refractometer is shown in Figure-4.1.

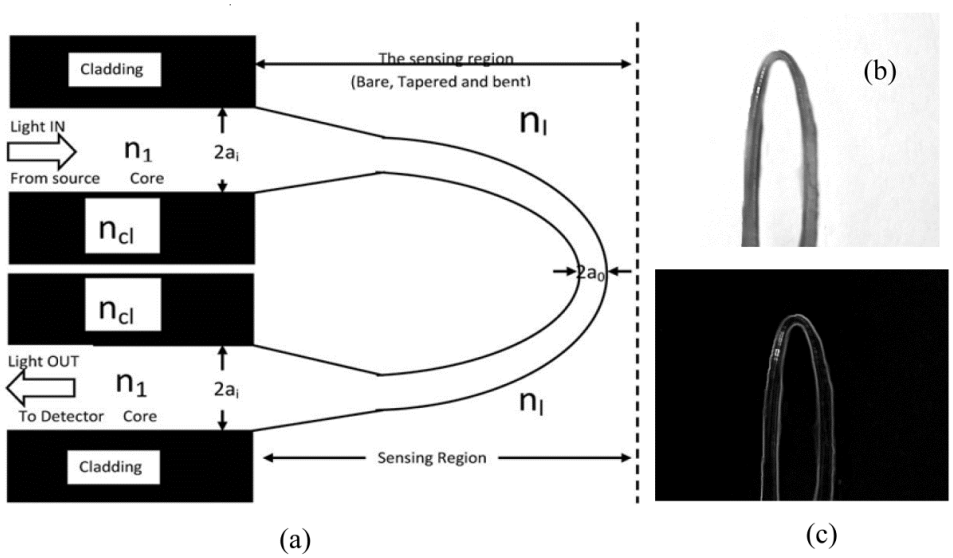

Fig.4.1: (a) The geometry of the proposed Refractometer, Inset (a) Image of the BTBMOF portion of the OFSP (b) Image of the BTBMOF portion of the OFSP after range-filtering method done at Matlab

The geometry of the proposed sensor shows that the expression of transmitted power of a propagating ray of light from the tapered zone to the fibre with reduced radius a_0 of the BTBMOF is given as (reference equation (2.24)).

$$P_b = P_0 \left[\frac{n_1^2 - n_l^2}{R^2(n_1^2 - n_{cl}^2)}\right] \tag{4.1}$$

where the terms in the expression carry the same meaning as given in chapter 2, section 2.4. The portion of the fibre with reduced radius a_0 of the BTBMOF is given the shape of a semicircular arc of fixed radius of curvature R'. An optical fibre suffers from transmission loss as the signal propagates through it. Thus for this bent portion of the fibre of length L, the expression of transmitted power of a propagating ray of light can be written as [68]:

$$P(L) = P_b e^{-0.2304\alpha_B L} \tag{4.2}$$

where α_B is the attenuation coefficient in nepers per unit length and can be attributed to macro bending effect, L is the length of the bent portion of the BTBMOF and $P(L)$ is the output power for the BTBMOF and P_b is the power coupled from the input of the fibre to the bare, tapered and bent portion of the fibre.

4.2.2 Attenuation Coefficient due to Bending in Bare and Tapered Multimode Fibre

For a macrobend multimode fibre, the attenuation coefficient due to bending (without any special case of flat or graded profile) as derived in chapter 2 section 2.3 is given by Gloge [26]-

$$\alpha_B = \frac{2\gamma^2(0)}{n_1 k_0} exp\left[-\frac{2}{3} n_1 k_0 R' \left(\frac{\gamma^2(0)}{n_1^2 k_0^2} - \frac{2a_0}{R'}\right)^{3/2}\right] \tag{4.3}$$

where $$\gamma(0) = \sqrt{\beta^2 - k_0^2 n_{cl}^2} \tag{4.4}$$

R' represents the radius of curvature, a_0 is the core radius of the proposed BTBMOF, n_1 and n_{cl} are the RI of core and cladding of the fibre respectively, β is the propagation constant and $k_0 = \omega/c$.

Substituting the term $\gamma^2(0)$ in equation (4.3), we have

$$\alpha_B = \frac{2(\beta^2 - k_0^2 n_{cl}^2)}{n_1 k_0} exp\left[-\frac{2}{3} n_1 k_0 R' \left(\frac{\beta^2 - k_0^2 n_{cl}^2}{n_1^2 k_0^2} - \frac{2a_0}{R'}\right)^{3/2}\right] \tag{4.5}$$

The propagation constant β is expressed in normalized form as

$$b = \frac{(\beta^2/k_0^2 - n_{cl}^2)}{n_1^2 - n_{cl}^2} \tag{4.6}$$

where, $0 \leq b \leq 1$ for a guided mode

dee

$$\Rightarrow \beta^2 - k_0^2 n_{cl}^2 = b k_0^2 (n_1^2 - n_{cl}^2) \tag{4.7}$$

Substituting the expression for $\beta^2 - k_0^2 n_{cl}^2$ in equation (4.7)

$$\alpha_B = \frac{2b k_0 (n_1^2 - n_{cl}^2)}{n_1} exp\left[-\frac{2}{3} n_1 k_0 R' \left(\frac{b k_0^2 (n_1^2 - n_{cl}^2)}{n_1^2 k_0^2} - \frac{2a_0}{R'}\right)^{3/2}\right] \tag{4.8}$$

In the proposed BTBMOF sensor, the cladding around the bent portion of the fibre has been removed and the bare, tapered and bent portion of the fibre is immersed in a liquid

with unknown RI ($i.e., n_{cl} = n_l$). Therefore, the attenuation coefficient for this portion of the fibre can be expressed as:

$$\alpha_B = \frac{2bk_0(n_1^2-n_l^2)}{n_1} exp\left[-\frac{2}{3}n_1k_0R'\left(\frac{bk_0^2(n_1^2-n_l^2)}{n_1^2k_0^2}-\frac{2a_0}{R'}\right)^{3/2}\right] \quad (4.9)$$

Combining equation (4.1) equation (4.2), gives

$$P(L) = P_0\left[\frac{n_1^2-n_l^2}{R^2(n_1^2-n_{cl}^2)}\right]e^{-0.2304\alpha_B L} \quad (4.10)$$

Now, expanding the exponential term and neglecting the higher order terms, equation (4.10) becomes

$$P(L) = P_0\left[\frac{n_1^2-n_l^2}{R^2(n_1^2-n_{cl}^2)}\right](1-0.2304\alpha_B L) \quad (4.11)$$

Substituting the expression for α_B from equation (4.8) in equation (4.11) gives

$$P(L) = P_o\left[\frac{n_1^2-n_l^2}{R^2(n_1^2-n_{cl}^2)}\right]\left[1-0.2304\,\frac{2bk_0(n_1^2-n_l^2)L}{n_1}\,exp\left\{-\frac{2}{3}n_1k_0R'\left(\frac{b(n_1^2-n_l^2)}{n_1^2}-\frac{2a_0}{R'}\right)^{3/2}\right\}\right] \quad (4.12)$$

If $R(=a_i/a_0), n_1, n_{cl}, R', K, k_0, b$ and L are kept constant (a_i is the radius of the uncladded, untapered and unbent portion of the fibre), then the transmitted power $P(L)$ can be expressed as

$$P(L) = P_0[K_1 - K_2n_l^2] \times \left[1-0.2304(K_3-K_4n_l^2)exp\{-K_5(b-K_6n_l^2-K_7)^{3/2}\}\right] \quad (4.13)$$

where,

$K_1 = \frac{n_1^2}{R^2(n_1^2-n_{cl}^2)}$, $K_2 = \frac{1}{R^2(n_1^2-n_{cl}^2)}$, $K_3 = \frac{2bn_1^2k_0L}{n_1}$, $K_4 = \frac{2bk_0L}{n_1}$, $K_5 = \frac{2}{3}n_1k_0R'$, $K_6 = \frac{b}{n_1^2}$ and $K_7 = \frac{2a_0}{R'}$

The term $\left[\frac{n_1^2-n_l^2}{R^2(n_1^2-n_{cl}^2)}\right]$ represents the effect of power coupled to the bare and tapered portion of BTBMOF.

The term $-0.2304\left[\frac{n_1^2-n_l^2}{R^2(n_1^2-n_{cl}^2)}\right]\frac{2bk_0(n_1^2-n_l^2)L}{n_1}\ exp\left\{-\frac{2}{3}n_1k_0R'\left(\frac{b(n_1^2-n_l^2)}{n_1^2}-\frac{2a_0}{R'}\right)^{3/2}\right\}$ represents the effect of bending, which is introduced at the tapered portion of the BTBMOF to enhance the sensitivity of the proposed BTBMOF.

4.3 DESCRIPTION OF THE OPTICAL-FIBRE SENSOR PROBE (OFSP)

The multimode optical fibre selected for the preparation of bare, tapered and bent refractiometer, has a dimension of 200/230 diameter (core diameter (μm)/ cladding diameter (μm)), i.e., core diameter is 200 μm and cladding thickness is 30 μm with coating diameter of 500μm. The RI of the core (n_1) and cladding (n_{cl}) of the fibre are 1.48 and 1.46 respectively. The length of the fibre is 20 cm. At the center of the fibre, a length measuring 25 mm is made open by removing the plastic jacket. After this, the cladding of this portion is removed mechanically by careful use of a sharp razor and this bare portion of the fibre is immersed into a solution of concentrated sulphuric acid for about 15-20 minutes. The uncladded portion of the fibre was then heated and pulled very carefully till the length become approximately 40 mm. Thus, bare portion of the fibre becomes tapered at its two ends. The length of the tapered portion is found to be approximately 10 mm. Therefore, the length of the fibre between the ends of the tapered potion of the fibre is approximately 20 mm. Thus, the tapered ratio of the fibre becomes 2.22.

To confirm the proper removal of cladding from the bare and tapered portion of the fibre, the procedure described in reference [46] is used. According to this procedure, the proper removal of cladding from the bare and tapered portion of the fibre can be confirmed. If the power of a laser beam that propagates through the bare and tapered portion of the fibre gets decreased with increase in RI value of a liquid applied around it, then it indicates the proper removal of the cladding. Sugar solutions with different RI have been used to verify

the proper removal of cladding from the bare and tapered portion of the fibre. The optical fibre is then placed inside two PVC tubes having radius 10 mm each, by keeping the bare and tapered portion exposed outside them.

The PVC tubes are filled with m-seal (a cementing material normally used for fixing water leakage through roof, water pipe etc) keeping the fibre at their centers. At one end of the PVC tube, the LDR is placed in such a way that the laser beam emerging out of fibre is incident on the LDR surface perpendicularly. Similarly, the position of the Diode Laser Source (with a pigtail) is fixed in the other end of the PVC tube with proper focusing. The use of pigtail ensures maintaining the proper focusing of Diode Laser source to the optical fibre sensor. After this, the PVC tubes are clubbed together so that the bare tapered portion of the optical fibre sensor gets a shape of a semicircular arc of fixed radius of curvature as shown in Figure-4.1.

The Diode Laser Source (Make Optochem International, 5mW power, 632nm), pigtail and the LDR (surface diameter 3.8mm) are also cemented with m-seal, so that their positions remain intact for ever. The resistance of a LDR has inverse-linear characteristics with the light incident on the LDR surface (in unit of Lux) in the range of 0.1-10,000 Lux. The power supply point of the Diode Laser Source is connected to one terminal of the LDR and they are connected to a stabilized 5V supply. The ground point of the Diode Laser Source is connected to ground point of the power supply through a resistance of 220 Ω. The other terminal of the LDR is connected to a series resistance to form a potential divider circuit. These three electrical wires are properly shielded with a metallic shield grounded wire to avoid influence of any external electric field around the sensor probe.

4.4 SCHEME OF THE INSTRUMENTATION SYSTEM

Fig. 4.3 shows the scheme adopted for the measurement of RI of an unknown liquid using the OFSP. The display unit interfaced to the microcontroller system consists of 16×2 (i.e. two rows having 16 character provisions) LCD display units. Switch *AR* (for air) and *TL* (for test liquid) are interfaced to pin PD.0 and PD.1 of Port D. These two switches are normally-open type. Therefore, under normal condition, the status of PD.0 and PD.1 will

be high. Whenever one of them is pressed, the status of PD.0 or PD.1 will be low depending upon the switch pressed. The status of these switches was utilized during the measurement steps. The flowchart for the microcontroller program is shown in Figure 4.4.

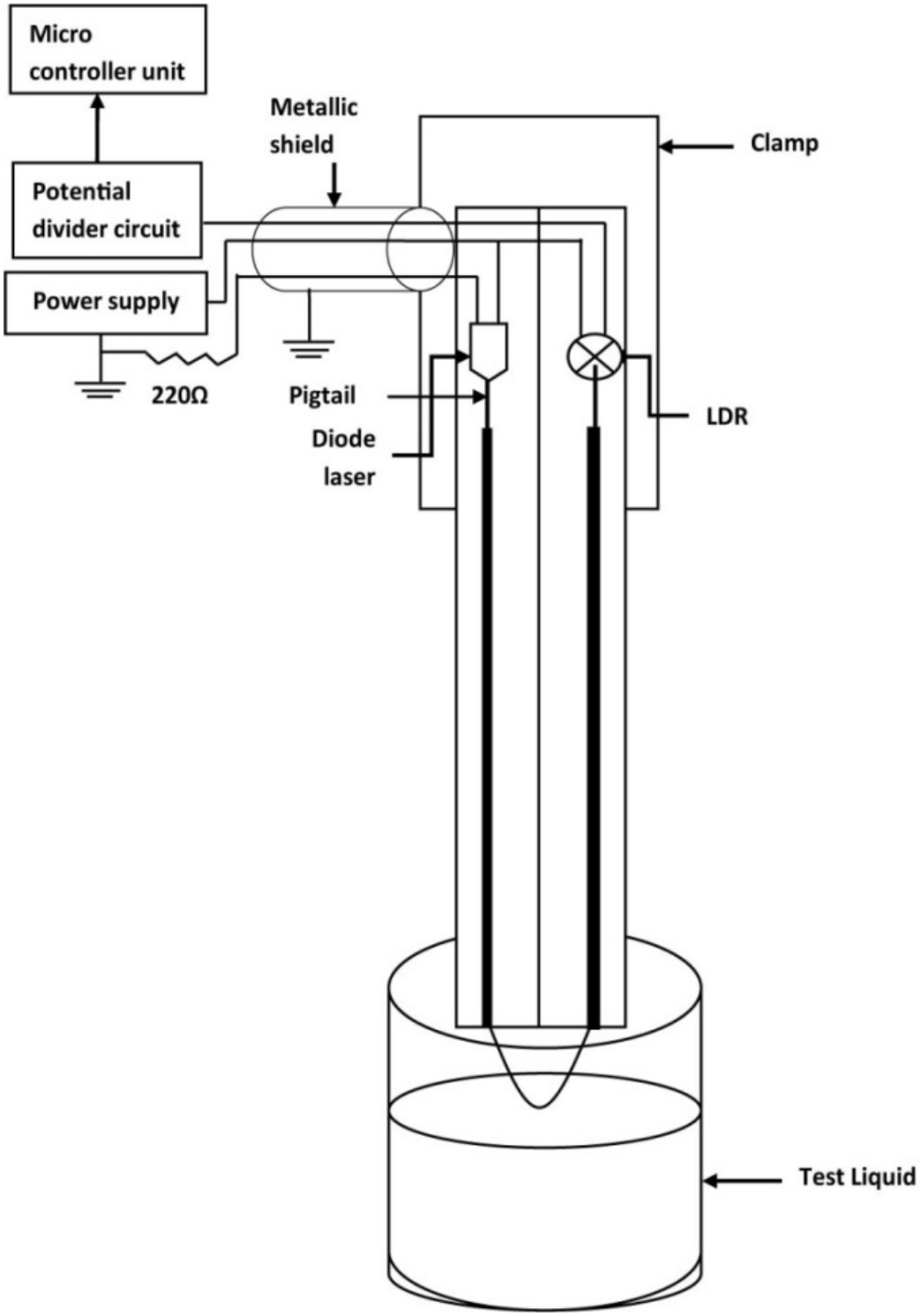

Fig. 4.2: Configuration of the measurement probe.

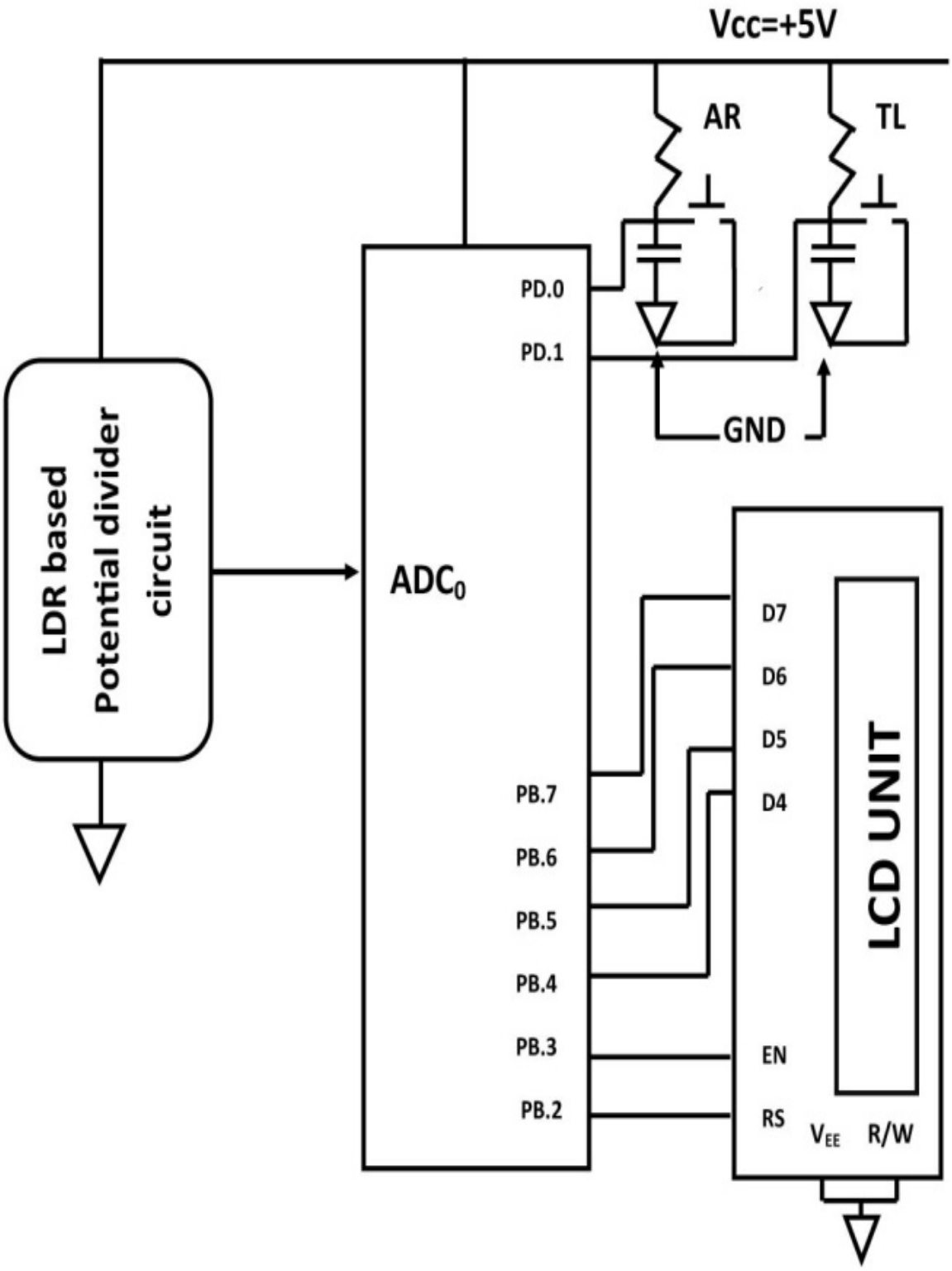

Fig. 4.3: Scheme adopted for measurement of RI of a liquid

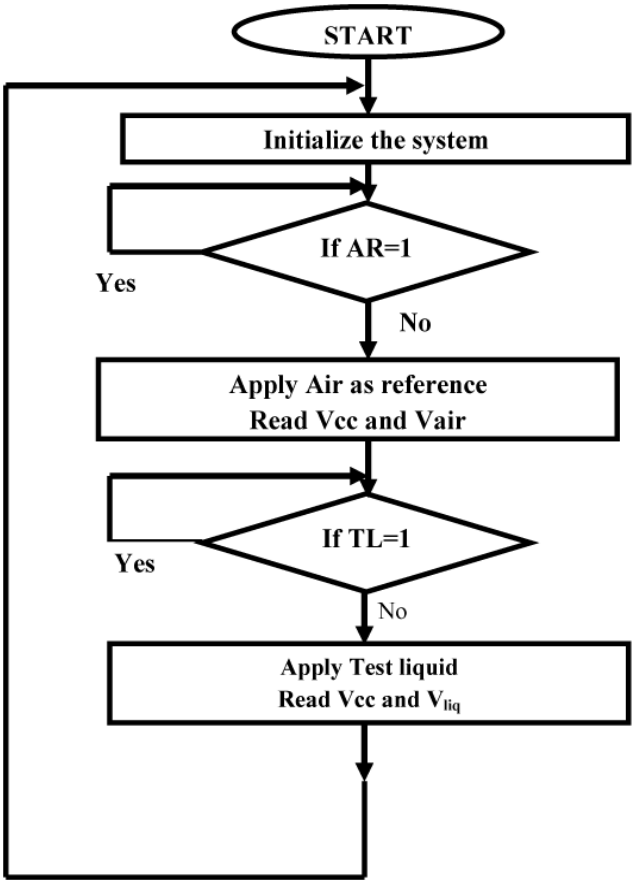

Fig.4.4: Flow chart for the Microcontroller program

The LDR is connected across a 5V DC supply with a series resistance with a fixed resistance (R_x =45kΩ) to form a potential divider circuit, as shown in Figure 4.5.

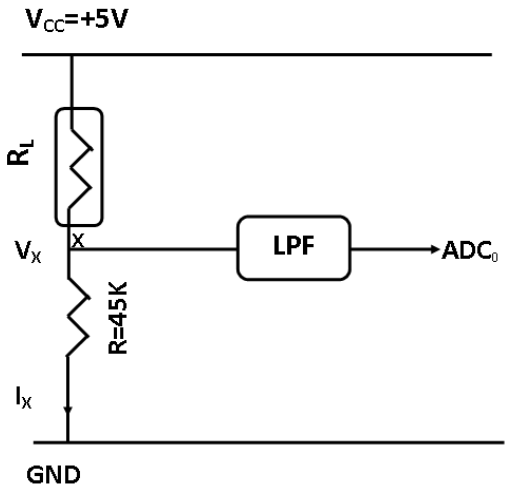

Fig. 4.5: LDR based potential divider circuit

where, R_x = 45 kΩ and Vcc = 5 Volts and I_x is the current passing through the circuit. Thus, I_x decreases with increase in the value of R_L. Therefore, V_x $(=I_x R_x)$ also decreased with increase in R_L. The value of R_L increases with increased in RI of the liquid which is applied around the sensing region of the OFSP.

The output voltage of the LDR based potential divider circuit can be expressed as-

$$V_x = I_x R_x = \frac{V_{cc}}{R_x + R_L} R_x \tag{4.14}$$

where R_L is the resistance of the LDR. The output voltage of the potential divider circuit V_x, decreases with increase in the value of R_{LDR}. Again, $R_L$increases with increase in the RI of the liquid in which the sensing region of the OFSP is immersed. The variation of power at the measurement point x can be expressed as

$$P_x = I_x^2 R_x = \left[\frac{V_{cc}}{R_x + R_L}\right]^2 R_x = \left(\frac{V_x^2}{R_x}\right) \tag{4.15}$$

The value of $R_x$and V_{cc} remain constant, therefore, P_x would be either inversely proportional to the $(R_x + R_{LDR})^2$ or proportional to V_x^2

$$P_x \propto \frac{1}{(R_x + R_L)^2} \propto V_x^2 \tag{4.16}$$

The LDR used in the potential divider circuit exhibits 500Ω, when it is exposed to the laser beam directly and shows 1 MΩ when the LDR is fully covered (i.e. no light is allowed to be incident on the LDR). It has been found that when the BTBMOF of the OFSP is exposed to air (i.e. condition for maximum power transfer through the BTBMOF), the resistance of the LDR is found to be 11 KΩ approximately. It is required to set the value of V_x around 4V, since V_x decreases with increase in the RI value of a liquid applied around the BTBMOF of the OFSP. Thus, the value of the resistance $R_x$should be 45 KΩ approximately to satisfy this condition.

The output from the potential divider circuit is then interfaced to the ADC0 (analogue input pin 0) of the ATmega 32 microcontroller via an LPF, having a cut-off frequency of 8 Hz.

P_0, (the power associated with the laser beam coupled through the tapered portion of the fibre) depends on the focusing arrangement of the laser beam launched from the diode laser source. Thus, depending upon the focusing arrangement of the laser to the input end of the fibre, the value of P_0 may vary from one OFSP to another OFSP

Two measurements are required to determine the refractive index of an unknown liquid. They are as follows:

Measurement-I: In this case, the bare, tapered and bent portion of the OFSP is exposed to air and power associated with laser beam at the output end of the fibre is measured. Power associated with the laser beam emerging out from the optical fibre can be represented as:

$$P(L)_{air} = P_0 \left[1 - 0.2304(K_3 - K_4 n_{air}^2) exp\left\{-K_5 (b - K_6 n_{air}^2 - K_7)^{3/2}\right\}\right] \quad (4.17)$$

Measurement-II: In this case, the bare, tapered and bent portion of the OFSP is immersed into the liquid under test (whose refractive index is unknown and assumed as,n_{liq}), and power associated with laser beam at the output end of the fibre can be expressed as:

$$P(L)_{liq} = P_0\left[K_1 - K_2 n_{liq}^2\right] \left[1 - 0.2304(K_3 - K_4 n_{liq}^2) exp\left\{-K_5 \left(b - K_6 n_{liq}^2 - K_7\right)^{3/2}\right\}\right] \quad (4.18)$$

Dividing equation (4.17) by equation (4.18), we have

$$\frac{P(L)_{air}}{P(L)_{liq}} = \frac{\left[1-0.2304(K_3-K_4 n_{air}^2) exp\left\{-K_5\left(b-K_6 n_{air}^2-K_7\right)^{3/2}\right\}\right]}{\left[K_1-K_2 n_{liq}^2\right] \left[1-0.2304(K_3-K_4 n_{liq}^2) exp\left\{-K_5\left(b-K_6 n_{liq}^2-K_7\right)^{3/2}\right\}\right]} \quad (4.19)$$

Now, using equation (4.16), the following equation is obtained

$$\frac{R_{liq}}{R_{air}} = \frac{V_{air}^2}{V_{liq}^2} = F_1 = \frac{\left[1-0.2304(K_3-K_4n_{air}^2)exp\left\{-K_5\left(b-K_6n_{air}^2-K_7\right)^{3/2}\right\}\right]}{\left[K_1-K_2n_{liq}^2\right]\left[1-0.2304(K_3-K_4n_{liq}^2)exp\left\{-K_5\left(b-K_6n_{liq}^2-K_7\right)^{3/2}\right\}\right]} \quad (4.20)$$

where F_1 is a function that describes the relationship between the output power associated with the Laser beam coming out of the fibre, expressed in terms of electrical voltage when the OFSP is kept in air and applied to the test liquid. Since the refractive index of air is known ((n_{air} =1.0003), the numerator part of equation (4.20) is a constant quantity. Thus F_1 is a measurement variable of the refractive index of the liquid surrounding the BTBMOF portion of the fibre. Thus the unknown RI can be measured by measuring the output voltages and taking the ratio of their squares when the BTBMOF is kept in air and immersed in test liquid.

4.5 MEASUREMENT PROCEDURE

Before starting the measurement, the BTBMOF portion of the optical-fibre sensor is cleaned by immersing it in methanol(CH_3OH). The cleansing and quick drying property of methanol makes it an ideal liquid for cleaning the sensing region of the fibre, after it is immersed in a liquid of unknown concentration (also unknown RI). To implement the measurement procedure, the status of the switches *AR* and *TL* are provided in the instrumentation system. The program starts with initializing the LCD unit and subsequently displaying the readiness to start the measurement procedure. It displays message to user to keep the optical probe in air and press switch *AR*. Once *AR* is pressed, the microcontroller samples the analog signal of the potential-divider circuit which represents the value of V_{air}. After this, the microcontroller displays a message to apply test liquid to sensing region of the OFSP and to press switch *TL*. Once *TL* is pressed, the microcontroller samples the analog signal of the potential-divider circuit which represents the value of V_{liq}. The user then uses methanol to properly clean the surface of the sensing region of the optical fibre. The microcontroller-based system uses these two readings to compute and display the refractive index of the liquid using point-to-point interpolation of the calibration curve, which is derived using the theoretical basis governed by equation (4.20). All measurement steps were carried out at the room temperature.

4.6 EXPERIMENTAL RESULTS AND DISCUSSION

To examine the characteristic behaviour of the OFSP, standard homogenous sugar solutions (w/v) were prepared by dissolving known weight of crystalline sugar in certain volume of water to prepare standard sugar solution and these solutions were used as test liquid for the experiment. To compare the performance of the bare and tapered refractometer given by Kumar, A., *et al*. [27] with the proposed OFSP having BTBMOF as sensor, the following steps are adopted.

Initially, while preparing the OFSP, the PVC tubes are filled with m-seal keeping the BTBMOF at their centers. The LDR and the Diode Laser Source are also cemented with m-seal so that their focusing alignment remains same. The PVC tubes are kept in the same axis (i.e., the bare and tapered portion (BTMOF) of the optical fibre is kept straight) to form a bare and tapered refractometer [27]. With this arrangement the OFSP is interfaced to the ATmega 32 microcontroller through potential-divider circuit and the low-pass filter (LPF).

This configuration of the OFSP has only bare and tapered refractometer as sensing element. Therefore, the power transfer in the bare and tapered refractometer can be expressed as

$$P(L) = P_0[K_1 - K_2 n_l^2] \tag{4.21}$$

Using the measurement steps described in section 4.4, the ratio of $\frac{V_{air}^2}{V_{liq}^2}$ for this refractometer can be expressed as

$$\frac{V_{air}^2}{V_{liq}^2} = F_2 = \frac{1}{\left[K_1 - K_2 n_{liq}^2\right]} \tag{4.22}$$

where F_2 is a function that describes the relation between the output power associated with the Laser beam coming out of the fibre, expressed in terms of electrical voltage when the OFSP is kept in air and applied to the test liquid. Thus F_2 is a measurement variable of the refractive index of the liquid surrounding the bare and tapered portion of the fibre.

After this, the PVC tubes are clubbed together so that the bare tapered portion of the optical fibre sensor gets a shape of a semicircular arc of fixed radius of curvature thus making the BTBMOF as shown in Figure-4.1. The values of V_{air} and V_{liq} are sampled by the ATmega 32 microcontroller system for the bare and tapered refractometer and the bare, tapered and bent refractometer with known percentage of sugar solutions and presented in Table-4.1

	For bare and tapered refractometer		**For bare, bent and tapered refractometer**		
per cent of Sugar	V_{air} **in Decimal**	V_{liq} **in Decimal**	V_{air} **in Decimal**	V_{liq} **in Decimal**	**Ideal RI n_l**
0	822	785	756	676	1.333
10	820	770	758	652	1.3478
20	819	749	758	620	1.3638
30	824	722	755	590	1.3811
40	820	678	756	550	1.3997
50	821	637	756	508	1.4200

Table 4.1: The experimental results for the OFSP with different percentages of sugar solution and corresponding refractive index values both for bare and tapered refractometer and bare, bent and tapered refractometer

A calibration curve for function F_1 (from Equation (4.20) and F_2 (From Equation (4.22)) vs the ideal refractive index of sugar solution (n_{liq}) is shown in Figure-3.7

The difference between the measurement variables F_1 and F_2 which gives the RI of the liquid for ranges from 0.15-0.55, for same RI range of sugar solutions as shown in Figure.4.6.

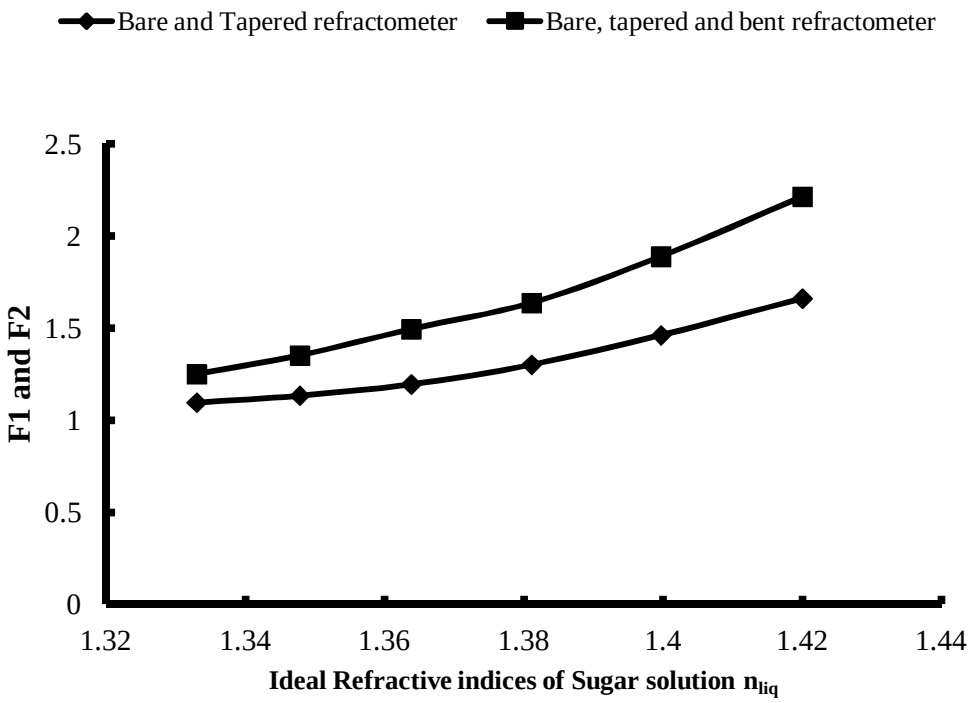

Fig. 4.6: Variation of function F1, F2 with ideal Refractive index n_{liq}

Figure 4.6 shows that the OFSP having BTBMOF is more sensitive as compared to that the refractometer having only bare and tapered optical fibre as sensor. In addition to it, the measurement procedure proposed allows calibration of the OFSP without measuring P_0, (power associated with the laser beam coupled through the tapered portion of the fibre). The BTBMOF portion of the OFSP is made structurally strong by fixing the fibre inside the PVC pipe filled with m-seal. Therefore, the geometry of the BTBMOF portion of the OFSP does not change, when it is cleaned with methanol solution.

Figure 4.6 also shows that the measurement variable F_1 varies no-linearly to the variation of refractive index of the sugar solution. Therefore, to calibrate the measurement variable F_1 with refractive index of the sugar solution, first order, second order interpolation and third order interpolation technique has been adopted using interpolation techniques in Matlab software.

The equation for calibration curve is found as:

$$n_{liq} = 1.227 + 0.08964\, F_1 \tag{4.23}$$

$$n_{liq} = 1.078 + 0.2686\, F_1 - 0.05166\, F_1^2 \tag{4.24}$$

$$n_{liq} = 0.9597 + 0.4835\, F_1 - 0.1789\, F_1^2 + 0.02456\, F_1^3 \tag{4.25}$$

Ethanol solution has been used as the calibrating liquid. The experimental results for the OFSP with different percentages of ethanol solution and corresponding refractive index values bare, tapered and bent refractometer is shown in Table.4.2

Sample used	**RI actual**	V_{air}	V_{liq}	$F_1 = V_{air}^2 / V_{liq}^2$
30 per cent Ethanol solution	1.3535	756	639	1.399722
40 per cent Ethanol solution	1.3583	755	630	1.436193
60 per cent Ethanol solution	1.3638	756	621	1.482042

Table.4.2: The experimental results for the OFSP with different percentages of ethanol solution and corresponding refractive index values using bare, tapered and bent refractometer

The measurement variable F_1 used to calculate the values of the RI of the ethanol solution which is used as calibration liquid and by applying equations 4.23, 4.24 and 4.25 the percentage error from known values of RI of ethanol solution is calculated for first, second and third order interpolation is shown in Table. 4.3.

Sample used	F_1	n_l (actual)	1st order		2nd order		3rd order	
			n_l (measured)	per cent Error	n_l (measured)	per cent Error	n_l (measured)	per cent Error
30 per cent Ethanol solution	1.399722	1.3535	1.3525	-0.076	1.3528	-0.0553	1.3533	-0.0138
40 per cent Ethanol solution	1.436193	1.3583	1.3557	-0.1884	1.3572	-0.0806	1.3578	-0.0334
60 per cent Ethanol solution	1.482042	1.3638	1.3599	-0.2896	1.3626	-0.0874	1.3633	-0.0388

Table 4.3: The Refractive index values of the different calibrated solutions using measurement variable F_1 and their corresponding percentage error values

Table 4.3 shows that the third-order interpolation technique has least error. Therefore this calibration technique is adopted for calibration of the instrumentation system.

It has again been observed that without the LPF, the reading of the LDR-based potential-divider circuit keeps fluctuating by -25 to +25 decimal values around the base value. This is due to the noise of the electronic devices and the high-frequency noise of the power supply which acts as the modifying input for the measurement system. The use of a passive LPF circuit (R-C circuit) with cut-off frequency of 8Hz brings down this fluctuation to -2 to +2 only.

4.7 CONCLUSION

In the present study an improvised optical fibre refractometer is fabricated using a bare, tapered and bent multimode optical fibre. The mathematical background for this refractometer was developed from the model of refractometer proposed by Kumar, A., *et al.* [27]. The mathematical theory is used as the basis for the working of the optical fibre in determining the change in refractive index of standard sugar solutions which has been used as the test liquid for testing the performance of the optical fibre refractometer.

A multimode optical fibre has been fabricated as an optical fibre sensor probe (OFSP). The sensing region of this probe is the bare, tapered and bent multimode optical fibre (BTBMOF). A microcontroller based Instrumentation system has also been developed for the implementation of the measurement of refractive index of liquid using the developed refractometer and correlating the measurement result with the theoretical result and its analysis. A laser beam propagates through BTBMOF, experiences macro bending effect, along with the power coupling effect that takes place at the bare and tapered portion of the portion the fibre. Two measurement methods were adopted for measuring the refractive index. In the first method, the BTBMOF portion of the OFSP is exposed to air and the measurement result is sampled by the microcontroller. In the second method the BTBMOF portion of the OFSP is exposed to the test liquid and the microcontroller samples the test result. Taking the ratio of the two samples, a function $F_1$was obtained which is a measure of refractive index of the test liquid. The function F_1 vs. ideal values of refractive index shows a rising non-linear curve. The curve for function F_1 infer that as the refractive index as the liquid refractive index increases (i.e. the liquid becomes more turbid), the voltage drop across the fixed resistance decreases. This could be attributed to the fact that as the refractive index of the liquid increases, more amount of light (leaky and cladding modes) leaks out into the test liquid. As a result, less amount of light reaches the LDR which increases its resistance. Since the LDR is a part of the potential divider circuit, there is less voltage drop across the fixed resistance which is sampled by the microcontroller. The sensitivity of the BTBMOF is then compared with the bare and tapered refractometer by immersing the bare and tapered portion of the fibre in standard sugar solution. By using the two measurement method as described before, another function F_2 was found out. By comparing the plot of F_1 and F_2 with the refractive index of the sugar solution, it was found that the sensitivity of the BTBMOF is more compared to that of bare and tapered refractometer. This is indicated by the Figure 4.6.

Since the curve obtained for function $F_1$is non linear, calibration equations of order one, two and three were used to relate the refractive index with the function F_1 using polynomial interpolation technique. Standard ethanol solutions were used as test liquid for the BTBMOF refractometer and the output of the measurement were tested in the three calibration equations. It was found that the third order interpolation equation has the least

error between the theoretical and experimental refractive index values, compared to first and second order.

It was also seen that the measurement procedure adopted for the microcontroller based Instrumentation system allows the calibration of the OFSP without measuring P_0, (power associated with the laser beam coupled through the tapered portion of the fibre) thus removing the hindrance of measuring the input power (for measuring refractive index of liquid) as is required in most refractometers.